2014

Element dependence of enhancement in optics emission from laser-induced plasma under spatial confinement

Changmao Li
Huazhong University of Science and Technology

Lianbo Guo
Huazhong University of Science and Technology

Xiangnan He
University of Nebraska-Lincoln

Zhongqi Hao
Huazhong University of Science and Technology

Xiangyou Li
Huazhong University of Science and Technology

See next page for additional authors

Authors
Changmao Li, Lianbo Guo, Xiangnan He, Zhongqi Hao, Xiangyou Li, Meng Shen, Xiaoyan Zeng, and Yongfeng Lu

JAAS

PAPER

View Article Online
View Journal | View Issue

Element dependence of enhancement in optics emission from laser-induced plasma under spatial confinement

Cite this: *J. Anal. At. Spectrom.*, 2014, **29**, 638

Changmao Li,[ab] Lianbo Guo,[ab] Xiangnan He,[b] Zhongqi Hao,[a] Xiangyou Li,[a] Meng Shen,[a] Xiaoyan Zeng[a] and Yongfeng Lu*[ab]

Received 18th November 2013
Accepted 2nd January 2014

DOI: 10.1039/c3ja50368b

www.rsc.org/jaas

In this study, the element dependence of spatial confinement effects in LIBS has been studied. Hemispheric cavities were used to confine laser-induced plasmas from aluminum samples with other trace elements. The enhancement factors were found to be dependent on the elements. Equations describing the element-dependent enhancement factors were successfully deduced from the local thermodynamic equilibrium conditions, which have also been verified by the experimental results. Research results show that enhancement factors in LIBS with spatial confinement depend on the temperature, electron density, and compression ratio of plasmas, and vary with elements and atomic/ionic emission lines selected. Generally, emission lines with higher upper level energies have higher enhancement factors. Furthermore, with enhancement factor of a spectral line, temperatures and electron densities of plasmas known, enhancement factors of all the other elements in the plasmas could be estimated by the equations developed in this study.

1 Introduction

Laser-induced breakdown spectroscopy (LIBS) has been proven to be a versatile analytical technique during the past decades. LIBS has many advantages,[1–5] such as the ability of detecting nearly all elements in any physical form (liquid, solid, gas, *etc.*), rapid and simultaneous multi-element detection, no or simple sample preparation, nearly nondestructive, capability of *in situ* and real-time analysis,[6–8] field deployment, and remote analysis for military[9–11] and space applications.[12] However, two drawbacks, including low sensitivity and poor reproducibility compared to other analytical techniques, such as inductively coupled plasma-optical emission spectroscopy (ICP-OES), have limited broad applications of LIBS.[13,14] Much effort has been made to improve its sensitivity and reproducibility, such as introduction of ambient gases,[15] multiple-pulse excitations,[16,17] resonant excitations,[18–20] magnetic confinements, spectra normalizations,[21] and spatial confinements.[22–28]

Among these methods described above, the spatial confinement is a cost-effective approach to improve the detection sensitivity of LIBS. Along with the generation and expansion of laser-induced plasma in an ambient gas, a shock wave is produced. If the shock wave encounters walls during its expansion, it would be reflected back by the walls to compress the expanding plasma, leading to an increase in electron density and plasma temperature, resulting in an enhancement of optical emission intensity. In recent years, the spatial confinement in LIBS has been studied by several groups. X. K. Shen *et al.*[22] used a series of round pipes to confine aluminium plasmas. The maximal enhancement factor of 9 was obtained at a pipe diameter of 10.8 mm. A. M. Popov *et al.*[23,24] reported the confinement effects of iron plasmas created in a small capped cylindrical chamber about 4 mm in diameter, with the limit of detections (LODs) 2–5 times better than those of free-expanding plasmas. Z. Wang *et al.*[25,29] used a cylindrical cavity of 1.5 mm in thickness and 3 mm in diameter to confine coal plasmas and reported an emission intensity enhancement with shot-to-shot fluctuation reduction. To confine laser-induced plasmas more uniformly, L. B. Guo *et al.*[26] used a hemispheric cavity to confine laser-induced steel plasmas. Strong enhancement of about 12 times was obtained on atomic manganese (1.05 wt%) lines around 403 nm. However, the previous research on the spatial confinement in LIBS reported so far mainly focused on improving enhancement effects using different kinds of cavities. The dependence of enhancement factors on plasma parameters, elements, and their emission lines has not been studied.

Therefore, the goal of this study was to investigate the element dependence of enhancement of optical emission in spatially confined LIBS. Intensity enhancement effects of multi-elements in aluminium plasmas spatially confined by hemispheric cavities were studied, to learn the dependence of enhancement factors on the plasma compression ratio, plasma temperature, plasma electron density, and different elements and their emission lines. Equations describing the element dependence have been successfully derived from the local

[a]*Wuhan National Laboratory for Optoelectronics (WNLO), Huazhong University of Science and Technology, Wuhan, Hubei 430074, PR China. E-mail: xyzeng@mail.hust.edu.cn; Fax: +86-27-87541427; Tel: +86-27-87541427*

[b]*Department of Electrical Engineering, University of Nebraska-Lincoln, Lincoln, NE 68588-0511, USA. E-mail: ylu2@unl.edu; Fax: +1-402-472-4732; Tel: +1-402-472-8323*

thermodynamic equilibrium (LTE) conditions, which have also been validated by the experimental data.

2 Experimental methods

The experimental setup used in this study is shown in Fig. 1, which was depicted in detail in our previous work.[26] Five polished Al hemispheric cavities with a top hole of 2 mm were used in the experiments, with diameters of 7.9, 9.5, 11.1, 12.7, and 15.9 mm, respectively. The cavity was placed tightly on the surface of an Al sample (SRM 1255b, NIST), which was mounted on a translation stage driven by a step-motor, moving in a direction perpendicular to the axis of the laser beam from a KrF excimer laser (Lambda Physik, Compex 205, wavelength: 248 nm, pulse duration: 23 ns). The focal spot of laser beam, located at the center of the cavity, was about 1.5×0.8 mm^2 in size, with a laser fluence of 10 J cm^{-2}. The spectrometer (Andor Shamrock 303i) equipped with a 2400 lines per mm grating and a 512×512 pixels intensified charge coupled device (ICCD) (Andor Tech., iStar, DH712), with a spectral resolution of about 0.05 nm, was used in the experiment. Prior to each acquisition, a number of pulses were applied to eliminate contamination on the sample surface.

The spectrum acquisition was carried on the delay times of maximum enhancement, which were 6, 9, 12, 16 and 23 μs, respectively, for the hemispheric cavities of 7.9, 9.5, 11.1, 12.7 and 15.9 mm. The gate width was 1 μs. Each acquisition was accumulated for 30 shots, repeated for 5 times at different places. Generally, the emission intensity of lines used in this study was defined as the maximum height of the peak (unit in counts) with background removed, except for Al I 394.4 nm which was defined as the area integral under the peak, to reduce the impact of self-absorption. The enhancement factor of a line was defined as the ratio of the emission intensity with confinement to that without confinement.

3 Results and discussion

3.1 Intensity enhancement effects of different elements in plasmas confined by a hemispheric cavity

Spectra of multi-elements from the spatially confined plasmas by the hemispheric cavity of 9.5 mm are shown in Fig. 2 and 3 (the black line), compared with that from the free-expanding plasma under the same conditions (the red line). As we can see, all of the lines have been enhanced greatly. The enhancement factors of some elements are summarized in Table 1, in which results from different spectra are separated by dashed lines. The error of enhancement factors is below 10%. As we can see in Table 1, enhancement factors of Cr I 359.35 nm and Ti I 363.55 nm are different evidently from that of other lines in Table 1. Furthermore, the difference between enhancement factors of Mg I 285.21 nm and Si I 288.16 nm or between that of Cu I 324.75 nm and Sn I 326.23 nm is not probably due to shot-to-shot variation as they were acquired simultaneously. Therefore, the intensity enhancement effects of spatial confinement are element dependent.

To further understand the intensity enhancement effects due to spatial confinement, the dependence of enhancement factors on plasma parameters, elements and lines selected has been studied.

3.2 Theoretical analyses of enhancement factors in spatial confinement

To investigate the dependence of enhancement factors on elements and lines selected, and plasma parameters, the enhancement factor due to spatial confinement has been derived from the LTE conditions.

Assume a condition that the laser ablation is stoichiometric and the compression of plasmas by the shockwave is uniform which means that the content of each element in plasmas with/without compression keeps the same with that in the target. Therefore, based on the LTE conditions, for an atomic emission induced by an electron transition of a species, the emitted line intensity (I) can be expressed as:[2,25]

$$I = FCN\left(\frac{1}{1+R}\right)\frac{gA}{U(T)}\mathrm{e}^{-\frac{E}{KT}} \quad (1)$$

$$R = \frac{n^{\mathrm{II}}}{n^{\mathrm{I}}} = \frac{2}{n}\frac{U^{\mathrm{II}}(T)}{U^{\mathrm{I}}(T)}\frac{(2\pi m_{\mathrm{e}}KT)^{1.5}}{h^3}\mathrm{e}^{-\frac{E_{\mathrm{ion}}-\Delta E_{\mathrm{ion}}}{KT}}. \quad (2)$$

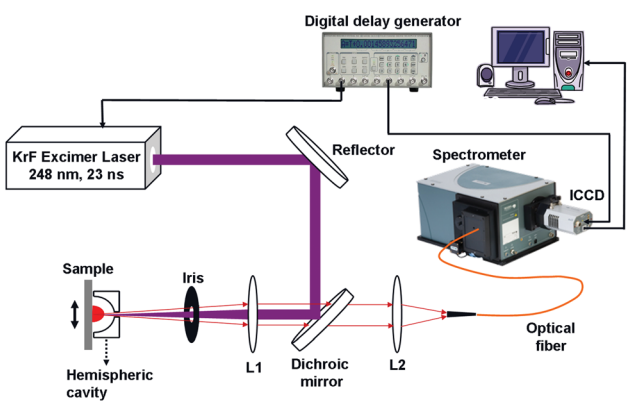

Fig. 1 Schematic diagram of the experimental setup.

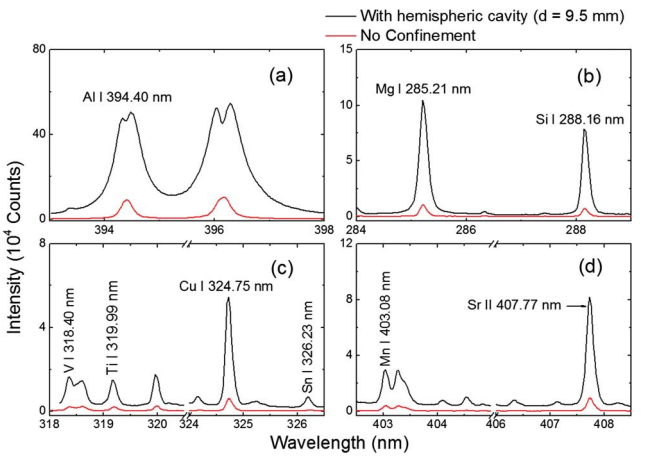

Fig. 2 Atomic emission spectra of aluminium plasma with confinement of hemispheric cavity (d = 9.5 mm) (black), and without confinement (red), at a delay time of 9 μs.

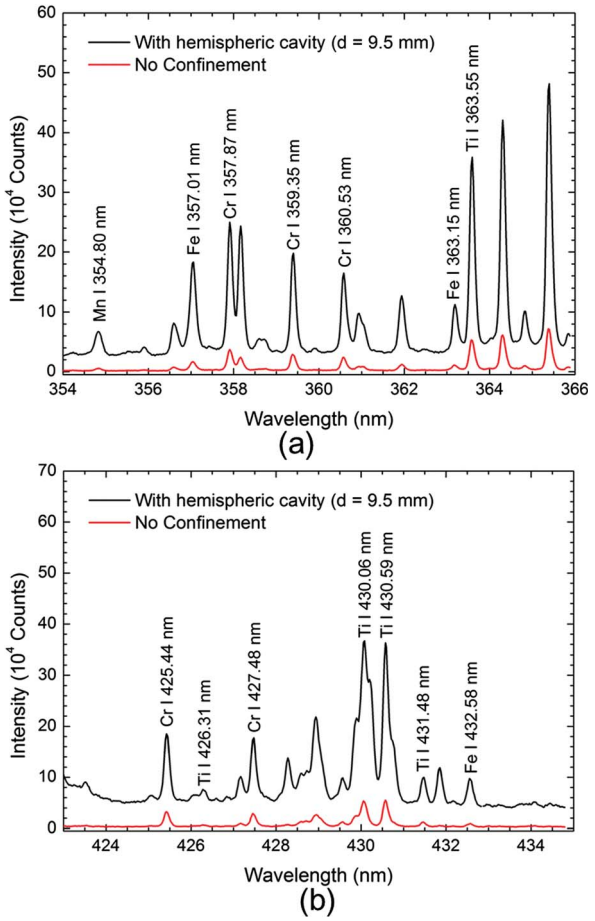

Fig. 3 Atomic emission spectra of aluminium plasma in (a) 354–366 nm and (b) 423–435 nm, with confinement of hemispheric cavity (d = 9.5 mm) (black), and without confinement (red). The gate delays were 9 μs.

Table 1 Enhancement factors of elements under confinement of a hemispheric cavity (d = 9.5 mm). Lines from different spectra are separated by dashed lines

Element	Line (nm)	Enhancement factor
Mg	Mg I 285.21	9.3
Si	Si I 288.16	10.4
Cu	Cu I 324.75	9
Sn	Sn I 326.23	10
Fe	Fe I 357.01	9
Cr	Cr I 359.35	6.2
Ti	Ti I 363.55	5.3
Sr	Sr II 407.77	8.7

In the equations, the parameters are: F – gain factor of the instrument, C – content of the element, N – total species number density of the plasma, R – ionization rate of this species at a plasma temperature T and an electron density n, g – degeneracy of the upper level of the transition, A – transition probability, $U(T)$ – partition function, E – the upper level energy of the excitation, K – Boltzmann constant, n^{I} and n^{II} – number densities of the neutral atoms and the ions at the first ionization state, respectively, E_{ion} – first ionization energy of the element, ΔE_{ion} – the ionization potential lowering factor with a typical value on the order of 0.1 eV, and h – Planck's constant.

In free-expanding plasmas, the plasma temperature is T_1, the electron density is n_1. Now, due to the spatial confinement imposed by a hemispheric cavity, the plasma temperature and electron density are both enhanced to T_2 and n_2, respectively. Therefore, the enhancement factor (M) of the line intensity can be derived from eqn (1):

$$M = \frac{N_2}{N_1}\frac{1+R(T_1,n_1)}{1+R(T_2,n_2)}\frac{U(T_1)}{U(T_2)}\mathrm{e}^{\frac{E}{K}\left(\frac{1}{T_1}-\frac{1}{T_2}\right)}. \quad (3)$$

The factor N_2/N_1 defined as the ratio of total number densities of the plasma with the confinement (N_2) to that without the confinement (N_1) corresponds to the compression ratio of the plasma by the shockwave, which is independent of elements in the plasma.

With the spatial confinement, the enhancement factor of line λ_{A} from element A is M_{A} and the enhancement factor of line λ_{B} from element B is M_{B}. Therefore, the ratio of the enhancement factors ($M_{\mathrm{A}}/M_{\mathrm{B}}$) could be derived from eqn (3):

$$\frac{M_{\mathrm{A}}}{M_{\mathrm{B}}} = X_{\mathrm{AB}}\frac{U_{\mathrm{B}}(T_2)/U_{\mathrm{B}}(T_1)}{U_{\mathrm{A}}(T_2)/U_{\mathrm{A}}(T_1)}\mathrm{e}^{\frac{E_{\mathrm{A}}-E_{\mathrm{B}}}{K}\left(\frac{1}{T_1}-\frac{1}{T_2}\right)}, \quad (4)$$

$$X_{\mathrm{AB}} = \frac{(1+R_{\mathrm{B}}(T_2,n_2))/(1+R_{\mathrm{B}}(T_1,n_1))}{(1+R_{\mathrm{A}}(T_2,n_2))/(1+R_{\mathrm{A}}(T_1,n_1))}. \quad (5)$$

If λ_{A} and λ_{B} are emitted by the species of the same element and in the same ionization state, eqn (4) could be simplified as:

$$\frac{M_{\mathrm{A}}}{M_{\mathrm{B}}} = \mathrm{e}^{\frac{E_{\mathrm{A}}-E_{\mathrm{B}}}{K}\left(\frac{1}{T_1}-\frac{1}{T_2}\right)}. \quad (6)$$

Now, the theoretically predicted enhancement factors due to spatial confinement have been fully described by eqn (3), (4) and (6). Eqn (3) reveals the factors determining the enhancement factor due to spatial confinement. Eqn (4) describes the dependence of enhancement factors on elements. Eqn (6) describes the dependence of enhancement factors on different emission lines of the same element and in the same ionization state. The three equations will be discussed and compared with the experimental results to prove their validity.

3.3 Experimental verification of enhancement factors in spatial confinement

3.3.1. Dependence of enhancement factors on plasma parameters. Based on eqn (3), the enhancement factors due to spatial confinement are dependent on the compression ratio of plasmas (N_2/N_1), the temperatures and electron densities of plasmas with/without confinement. In order to understand the dependence more clearly, eqn (3) can be rewritten as:

$$\begin{cases} M = \dfrac{N_2}{N_1}\dfrac{1+\dfrac{2}{n_1}W(T_1)}{1+\dfrac{2}{n_2}W(T_2)}\dfrac{U(T_1)}{U(T_2)}\mathrm{e}^{\frac{E}{K}\left(\frac{1}{T_1}-\frac{1}{T_2}\right)} \\ W(T) = \dfrac{U^{\mathrm{II}}(T)}{U^{\mathrm{I}}(T)}\dfrac{(2\pi m_{\mathrm{e}}KT)^{1.5}}{h^3}\mathrm{e}^{-\frac{E_{\mathrm{ion}}-\Delta E_{\mathrm{ion}}}{KT}} \end{cases}. \quad (7)$$

Generally, the influences of plasma temperature (T_2, T_1) and electron density (n_2, n_1) are convoluted together. Electron density has a weaker impact on the enhancement factor compared to that of the plasma temperature. In contrast, the compression ratio of plasma (N_2/N_1), a constant for all the species in the plasma, has a linear relationship with the enhancement factor (M).

3.3.2. Validation of LTE conditions. In order to validate eqn (4) and (6), the temperatures and electron densities of plasmas with/without confinement are needed. The temperatures of plasmas with/without spatial confinement used in calculation were deduced from the emission intensity ratio of Ti I 426.313 nm and Ti I 430.591 nm following the formula below.[2]

$$\frac{I_1}{I_2} = \frac{g_1A_1\lambda_2}{g_2A_2\lambda_1}\mathrm{e}^{-\frac{E_1-E_2}{KT}}. \quad (8)$$

The parameters of both the Ti lines are summarized in Table 2. The calculated temperatures of the plasmas with/without confinement using hemispheric cavities of 7.9, 9.5, 11.1, 12.7, and 15.9 mm are shown in Table 3.

The electron densities of plasmas with/without spatial confinement were calculated from the Stark broadening of Si I 390.55 nm, based on the formula below:[2]

$$\Delta\lambda_{\mathrm{FWHM}} \approx 2 \times 10^{-16} w N_{\mathrm{e}}. \quad (9)$$

The errors of plasma temperatures and electron densities in Table 3 are 5% and 10%. As shown in Table 3, the plasma temperatures were in the range of 4000–7000 K. For a conservative estimation, the lowest electron density required for LTE by the McWhirter criterion[2] which is just necessary is about 3×10^{16} cm^{-3}. The electron densities of plasmas were in the range of 2.2×10^{17} to 6.7×10^{17} cm^{-3}, satisfying the criterion.

The LTE conditions can be considered to be fully satisfied when the diffusion length during the relaxation time is much shorter than the plasma diameter.[30] For this study, the diffusion lengths were smaller than 9.4 μm. In contrast, the diameters of plasmas were larger than 2 mm, which are 2–3 orders larger than the diffusion length. Therefore the LTE conditions have been fully satisfied.

3.3.3. Dependence of enhancement factors on different emission lines of the same element. The dependence of enhancement factors on emission lines from the species of the same element and in the same ionization state is described by eqn (6).

For lines emitted from the same excited state ($E_{\mathrm{A}} = E_{\mathrm{B}}$), the enhancement factors should be equal to each other. To verify this conclusion, intensity enhancement of Cr, Fe, and Ti lines from the aluminium plasmas confined by the hemispheric cavity of 9.5 mm was examined in two regions of 354–366 nm and 423–435 nm, as shown in Fig. 3(a) and (b). The selected lines, the corresponding upper level energies, and enhancement factors are summarized in Table 4. As we can see, enhancement factors of the three lines of Cr (the same for Fe and Ti) are similar due to similar upper level energies. It is also necessary to mention that the enhancement factor of Ti I 363.55 nm (in Table 1) was about 5.3 which is apparently lower than that of Ti I 430.06 nm (6.5) as the former line has a lower upper level energy (about 3.4 eV). Therefore, the lines with the same upper level energy (E_{upper}) have the same enhancement factor.

For lines emitted from different excited states of an element, the enhancement factors are different from each other. For lines having higher upper level energies, the enhancement factors are higher. To verify this conclusion, intensity enhancement effects of Cr I 359.35 nm ($E_{\mathrm{upper}} = 3.4495$ eV) and Cr I 425.44 nm ($E_{\mathrm{upper}} = 2.9137$ eV) by hemispheric cavities of 7.9, 9.5, 11.1, 12.7, and 15.9 mm have been studied. The enhancement factors for both emission lines of Cr I 359.35 nm (λ_{A}) and 425.44 nm (λ_{B}) and the ratio of the two enhancement factors ($M_{\mathrm{A}}/M_{\mathrm{B}}$) are summarized in Table 5. The theoretical

Table 2 Parameters of two neutral titanium lines for plasma temperature determination

Wavelength (nm)	E (eV)	gA (10^8/s)
Ti I 426.313	4.795	6.674
Ti I 430.591	3.727	8.050

Table 3 Plasma temperatures and electron densities with/without confinement using hemispheric cavities

Diameter of cavity (mm)	Plasma temperature ($\times 10^3$ K)		Electron density ($\times 10^{17}$ cm^{-3})	
	With cavity	Without cavity	With cavity	Without cavity
7.9	6.8	5.5	6.7	3.6
9.5	6.4	5.2	6.5	2.9
11.1	6.0	4.9	6.2	2.6
12.7	5.8	4.4	5.6	2.5
15.9	5.4	4.1	5.7	2.2

Table 4 Enhancement factors of elements Ti, Fe & Cr in plasma with the hemispheric cavity of 9.5 mm

Line (nm)	E_{upper} (eV)	Enhancement factor
Cr I 357.87	3.4638	6.3
Cr I 359.35	3.4495	6.2
Cr I 360.53	3.4382	6.1
Fe I 357.01	4.3865	9.0
Fe I 363.15	4.3714	8.9
Fe I 432.58	4.4736	9.4
Ti I 430.06	3.7083	6.5
Ti I 430.59	3.7273	6.2
Ti I 431.48	3.7089	6.6

Table 5 Ratio (M_A/M_B) of enhancement factors of Cr I 359.35 nm (E_{upper} = 3.4495 eV) and Cr I 425.44 nm (E_{upper} = 2.9137 eV), compared with the theoretical value by eqn (6)

	Experimental			Theoretical
Diameter of cavity (mm)	M_A (Cr 359.35 nm)	M_B (Cr 425.44 nm)	M_A/M_B	M_A/M_B
7.9	5.3	4.3	1.23	1.24
9.5	6.2	4.9	1.27	1.25
11.1	5.7	4.5	1.27	1.26
12.7	7.4	5.2	1.42	1.41
15.9	10.2	6.8	1.50	1.44

values of M_A/M_B have also been calculated by eqn (6), summarized in Table 5 for comparison.

From Table 5, it is obvious that both the experimental and the theoretical values of M_A/M_B agree with each other well. Therefore, eqn (6) has been verified using the experimental results. Enhancement factors of other lines of an element can be estimated using eqn (6) when the enhancement factor of a line of the element and plasma temperatures are known.

3.3.4. Dependence of enhancement factors on lines of different elements. The dependence of enhancement factors on different elements is described by eqn (4). Ti I 430.06 nm (E_{upper} = 3.7083 eV) and Cr I 425.44 nm (E_{upper} = 2.9137 eV) in Fig. 3(b) have been chosen to study this complex dependence numerically. The enhancement factors of Ti I 430.59 nm and Cr I 425.44 nm in the aluminium plasmas confined by hemispheric cavities, and the ratios of the two enhancement factors (M_A/M_B) are summarized in Table 6.

To compare with the experimental values, the theoretical values of M_A/M_B are also calculated by eqn (4), in which the temperatures and electron densities of plasma with/without confinement were taken from those in Table 3. The partition function $U(T)$ can be attained from NIST.[31]

The results of theoretical values of M_A/M_B are summarized in Table 6. From Table 6, the experimental and theoretical values of M_A/M_B agree with each other well. Therefore, eqn (4) has been verified using the experimental results. Based on a known enhancement factor of a spectral line, eqn (4) and (6) can be used to estimate enhancement factors of other elements/lines in the spatially confined plasmas without additional experiments.

Table 6 Ratio (M_A/M_B) of enhancement factors of Ti I 430.06 nm (E_{upper} = 3.7083 eV) and Cr I 425.44 nm (E_{upper} = 2.9137 eV), compared with the theoretical value by eqn (4)

	Experimental			Theoretical
Diameter of cavity (mm)	M_A (Ti 430.06 nm)	M_B (Cr 425.44 nm)	M_A/M_B	M_A/M_B
7.9	5.7	4.3	1.3	1.3
9.5	6.5	4.9	1.3	1.4
11.1	6	4.5	1.3	1.4
12.7	8.2	5.2	1.6	1.6
15.9	11.5	6.8	1.7	1.7

4 Conclusions

In summary, intensity enhancement effects of Al, Mg, Si, V, Ti, Cu, Sn, Mn and Sr in spatially confined aluminium plasmas were studied by spatially confined LIBS, showing that the enhancement factors are dependent on elements. Equations describing the dependence of enhancement factors in spatial confinement on plasma parameters and elements/lines selected have been successfully derived from the LTE conditions and validated by the experimental results. The results show that enhancement factors due to spatial confinement are dependent on the plasma temperature, plasma electron density, and compression ratios of the plasma. They vary with the elements/lines selected. Generally, lines emitted from the same excited state of an element have the same enhancement factors. Lines with higher upper level energies have higher enhancement factors. With the equations developed in this study, enhancement factors of other elements/lines in the plasma can be estimated when the enhancement factors of a line, plasma temperatures, and plasma electron densities with/without confinement are known.

Acknowledgements

This research was financially supported by the National Special Fund for the Development of Major Research Equipment and Instruments (no. 2011YQ160017) of China and by the National Natural Science Foundation of China (no. 51128501).

Notes and references

1 D. A. Rusak, B. C. Castle, B. W. Smith and J. D. Winefordner, *Crit. Rev. Anal. Chem.*, 1997, **27**, 257–290.
2 J. P. Singh and S. N. Thakur, *Laser-Induced breakdown Spectroscopy*, Elsevier Science, Oxford, 2006.
3 D. A. Cremers and R. C. Chinni, *Appl. Spectrosc. Rev.*, 2009, **44**, 457–506.
4 D. W. Hahn and N. Omenetto, *Appl. Spectrosc.*, 2010, **64**, 335A–366A.
5 D. W. Hahn and N. Omenetto, *Appl. Spectrosc.*, 2012, **66**, 347–419.
6 J. P. Singh, F. Y. Yueh, H. S. Zhang and R. L. Cook, *Process Control Qual.*, 1997, **10**, 247–258.
7 J. E. Carranza, B. T. Fisher, G. D. Yoder and D. W. Hahn, *Spectrochim. Acta, Part B*, 2001, **56**, 851–864.
8 R. S. Harmon, F. C. De Lucia, A. W. Miziolek, K. L. McNesby, R. A. Walters and P. D. French, *Geochem.: Explor., Environ., Anal.*, 2005, **5**, 21–28.
9 F. C. DeLucia, A. C. Samuels, R. S. Harmon, R. A. Walters, K. L. McNesby, A. LaPointe, R. J. Winkel and A. W. Miziolek, *IEEE Sens. J.*, 2005, **5**, 681–689.
10 B. Salle, P. Mauchien and S. Maurice, *Spectrochim. Acta, Part B*, 2007, **62**, 739–768.
11 F. C. De Lucia, J. L. Gottfried, C. A. Munson and A. W. Miziolek, *Appl. Opt.*, 2008, **47**, G112–G121.
12 B. Salle, J. L. Lacour, P. Mauchien, P. Fichet, S. Maurice and G. Manhes, *Spectrochim. Acta, Part B*, 2006, **61**, 301–313.

13 P. Fichet, M. Tabarant, B. Salle and C. Gautier, *Anal. Bioanal. Chem.*, 2006, **385**, 338–344.
14 W. Q. Lei, J. El Haddad, V. Motto-Ros, N. Gilon-Delepine, A. Stankova, Q. L. Ma, X. S. Bai, L. J. Zheng, H. P. Zeng and J. Yu, *Anal. Bioanal. Chem.*, 2011, **400**, 3303–3313.
15 A. J. Effenberger and J. R. Scott, *Sensors*, 2010, **10**, 4907–4925.
16 V. I. Babushok, J. F. C. DeLucia, J. L. Gottfried, C. A. Munson and A. W. Miziolek, *Spectrochim. Acta, Part B*, 2006, **61**, 999–1014.
17 X. N. He, W. Hu, C. M. Li, L. B. Guo and Y. F. Lu, *Opt. Express*, 2011, **19**, 10997–11006.
18 X. K. Shen and Y. F. Lu, *Appl. Opt.*, 2008, **47**, 1810–1815.
19 S. L. Lui and N. H. Cheung, *Anal. Chem.*, 2005, **77**, 2617–2623.
20 W. L. Yip and N. H. Cheung, *Spectrochim. Acta, Part B*, 2009, **64**, 315–322.
21 Z. Wang, L. Z. Li, L. West, Z. Li and W. D. Ni, *Spectrochim. Acta, Part B*, 2012, **68**, 58–64.
22 X. K. Shen, J. Sun, H. Ling and Y. F. Lu, *J. Appl. Phys.*, 2007, **102**, 093301.
23 A. M. Popov, F. Colao and R. Fantoni, *J. Anal. At. Spectrom.*, 2009, **24**, 602–604.
24 A. M. Popov, F. Colao and R. Fantoni, *J. Anal. At. Spectrom.*, 2010, **25**, 837–848.
25 Z. Wang, Z. Y. Hou, S. L. Lui, D. Jiang, J. M. Liu and Z. Li, *Opt. Express*, 2012, **20**, A1011–A1018.
26 L. B. Guo, C. M. Li, W. Hu, Y. S. Zhou, B. Y. Zhang, Z. X. Cai, X. Y. Zeng and Y. F. Lu, *Appl. Phys. Lett.*, 2011, **98**.
27 L. B. Guo, W. Hu, B. Y. Zhang, X. N. He, C. M. Li, Y. S. Zhou, Z. X. Cai, X. Y. Zeng and Y. F. Lu, *Opt. Express*, 2011, **19**, 14067–14075.
28 L. B. Guo, B. Y. Zhang, X. N. He, C. M. Li, Y. S. Zhou, T. Wu, J. B. Park, X. Y. Zeng and Y. F. Lu, *Opt. Express*, 2012, **20**, 1436–1443.
29 Z. Hou, Z. Wang, J. Liu, W. Ni and Z. Li, *Opt. Express*, 2013, **21**, 15974–15979.
30 G. Cristoforetti, A. De Giacomo, M. Dell'Aglio, S. Legnaioli, E. Tognoni, V. Palleschi and N. Omenetto, *Spectrochim. Acta, Part B*, 2010, **65**, 86–95.
31 http://physics.nist.gov/PhysRefData/ASD/levels_form.html.